学位論文

参考論文１、参考論文２、参考論文３、参考論文４、参考論文５

博士論文

Pericyte-specific deletion of Ninjurin1 induces fragile vasa vasorum formation and enhances intimal hyperplasia of injured vasculature.

周細胞特異的 Ninjurin1 欠損は傷害血管において血管外膜毛細血管を脆弱化し、内膜肥厚を増悪させる。

American journal of physiology heart and circulatory physiology

受理（articles in press）

旭川医科大学大学院医学系研究科博士課程臨床研究者コース専攻

著者名　堀内　至

共著者名

鹿野耕平、蓑島暁帆、早坂太希、山内敦司、竜川貴光、松尾梨沙、

吉田有里、富田唯、鹿原真樹、中川直樹、竹原有史、長谷部直幸、川辺淳一

Abstract

Adventitial abnormalities including enhanced vasa vasorum malformation are associated with development and vulnerability of atherosclerotic plaque. However, the mechanisms of vasa vasorum malformation and its role in vascular remodeling have not been fully clarified. We recently reported that Ninjurin-1 (Ninj1) is a crucial adhesion molecule for pericytes to form matured neovessels. The purpose is to examine if Ninj1 regulate adventitial angiogenesis and affects the vascular remodeling of injured vessels using pericyte-specific *Ninj1* deletion mouse model.

Mouse femoral arteries were injured by insertion of coiled wire. Four weeks after vascular injury, fixed arteries were decolorized. Vascular remodeling, including intimal hyperplasia and adventitial microvessel formation were estimated in three-dimensional view. Vascular fragility, including blood leakiness was estimated by extravasation of FITC-lectin or -dextran from microvessels. Ninj1 expression was increased in pericytes in response to vascular injury. NG2-CreER/*Ninj1*^{loxp} mice were treated with tamoxifen (Tam) to induce deletion of *Ninj1* in pericyte (Ninj1KO). Tam-treated-NG2-CreER or Tam-nontreated NG2-CreER/*Ninj1*^{loxp} mice were used as controls. Intimal hyperplasia was significantly enhanced in *Ninj1*KO compared with controls. Vascular leakiness was significantly enhanced in *Ninj1*KO. In *Ninj1*KO, the number of infiltrated macrophages in adventitia was increased, along with the expression of inflammatory cytokines.

In conclusion, deletion of *Ninj1* in pericytes induces the immature vasa vasorum formation of injured vasculature and exacerbates adventitial inflammation and intimal hyperplasia. Thus, Ninj1 contributes to the vasa vasorum maturation in response to vascular injury, and to reduction of vascular remodeling.

Introduction

The vasa vasorum is a microvessel network in the adventitia of large vessels that supplies nutrients and oxygen to the adventitia and outer medial layer of parent vessels (34). Under pathological conditions, such as atherosclerosis, neovascularization of the vasa vasorum is enhanced by vessel wall thickening and adventitial inflammation (26). Inflammatory cell accumulation is observed in the adventitia of atherosclerotic vessel walls (18). Accordingly, to oppose the concept that inflammatory cells infiltrate vessel walls, a new concept, known as the outside-in theory, whereby vascular inflammation and neoangiogenesis begin in the adventitia, precede intimal thickening, and advance to the media/intima has been proposed (18, 26).

A growing body of evidence suggests that expansion as well as its structural and functional impairment in the vasa vasorum, including fragile and leaky microvessels, are closely associated with atherosclerotic plaque progression, and play a pivotal role in the outside-in theory of atherosclerosis (6, 14, 26, 31). Inherent vasa vasorum leak enables entry of inflammatory cells, red blood cells, and lipoproteins within plaques, and intraplaque hemorrhages are an important trigger for plaque progression, instability, and rupture (6, 31, 33, 37). Furthermore, fragile neovessels reduce perfusion flow, regardless of intraplaque vasa vasorum expansion, and contribute to plaque ischemia and growth (29). Thus, normalization of impaired vasa vasorum is an attractive therapeutic strategy, as opposed to mere anti-angiogenesis therapy. However, the pathophysiological mechanism of vasa vasorum angiogenesis remains to be clarified because of limited knowledge about vascular maturation and lack of appropriate methods to observe arterial wall microvessels.

Nerve-injury induced protein 1 (Ninjurin-1) was originally identified as a cell-surface adhesion molecule expressed in nervous tissues in response to nerve injury (2).

Ninjurin-1 is widely expressed in several tissues 85 and cells, and is involved in diverse pathophysiological conditions (17, 27, 39). Recently, we reported that Ninjurin-1 expression in pericytes is induced in response to ischemia, and mediates neovessel maturation through the association of endothelial cells and pericytes (19, 20). In this study, we three-dimensionally observed adventitial microvessel formation in injured arteries and investigated the role of Ninjurin-1 in vasa vasorum formation and vascular remodeling in response to vascular injury using pericytes-specific Ninjurin-1 deletion mouse model.

Methods and Materials

Animals. All experiments involving animals were performed according to protocols approved by the Animal Care and Use Committee of Asahikawa Medical University. Mice (C57BL/6, 12-18-week-old males) were housed in a temperature and light-controlled facility and fed normal chow. Wild type mice; neuron-glial antigen 2 (NG2)-DsRed mice, which express DsRed (red fluorescence) under the control of an NG2 promoter; and NG2-CreER/*Ninj1*^{loxP} mice were generated by crossing NG2-CreER transgenic mice as reported previously (20, 34). NG2-CreER/*Ninj1*^{loxP} mice were treated with tamoxifen (Sigma-Aldrich, St. Louis, MO) at a dosage of 100 mg/kg of body weight via oral administration for 5 consecutive days to create pericytes-specific *Ninjurin-1* (*Ninj1*) knockout mice (*Ninj1* KO). Tamoxifen-treated NG2-CreER mice and vehicle (corn oil)-treated NG2-CreER/*Ninj1*^{loxP} mice were allocated to control group 1 and 2, respectively.

Wire-mediated vessel injury model. A wire-mediated endovascular injury mouse model was utilized as described previously (15, 38). Briefly, under 2% isoflurane anesthesia, the left femoral artery was exposed and the muscular branch artery that bifurcates from the

femoral artery was cut transversally before inserting a straight coiled wire (0.38 mm in diameter, COOK, Bloomington, IN) from the muscular branch artery into the femoral artery. The wire was left for 1 min, and the branch artery was tied using 10-0 nylon suture. Mice were regularly housed for 4 weeks after surgery.

Intravital blood vessel labeling fluorescein isothiocyanate-conjugated-lectin. Mice were injected with 300 μl of fluorescein isothiocyanate (FITC)-labeled/rhodamine-labeled lectin (Griffonia Simplicifolia lectin: 100 μg/ml phosphate-buffered saline (PBS); Vector Laboratories, Burlingame, CA) or FITC-labeled dextran (15 mg/ml PBS; FD70S [70kDa], Sigma-Aldrich) via the tail vein under anesthesia to enable visualization of blood vessels by lectin binding. After circulating the lectin in the vasculature for 10 min, the chest was opened and the vasculature was perfused from the left ventricle with 20 ml of 2% paraformaldehyde (PFA) in PBS. The femoral arteries were then removed together with the surrounding perivascular fatty tissue and femoral veins and nerves, and soaked in 4% PFA at 4 ℃ for 2 hours.

Immunohistological analyses. PFA-fixed samples were embedded in Tissue-Tek Optimal Cutting Temperature Compound and sectioned to10 μm. Short axis sections of femoral arteries were treated in 4% PFA for 10 min and immersed sequentially in PBS containing 0.3% Triton-X (PBS-T) and blocking solution (PBS-T containing 0.5% bovine serum albumin) for 60 min at room temperature. The tissue sections were incubated with 1:100 anti-CD31 (rat monoclonal IgG, ab7388, Abcam, Cambridge, UK) and 1:100 anti-Ninj1 (rabbit polyclonal IgG, ab213695, Abcam). Invaded macrophages within vascular walls were immunostained with 1:100 anti-F4/80 antibody (Rat IgG, 14-4801-82, eBioscience) and visualized with Alexa Fluor 594 secondary antibody (goat anti-rat IgG,

Thermo Fisher Scientific, Waltham, MA). Nuclei were counterstained with Hoechest 33342 (H3570, Invitrogen, Waltham, MA). Three observation points (40x) within adventitial areas were randomly selected, and F4/80-positive macrophages were counted using a fluorescence microscope (BZ-X710, Keyence, Osaka5 Japan) and calculated as cell number per area.

Whole-mount imaging analyses. PFA-fixed samples were incubated sequentially in PBS-T and blocking solution overnight at 4℃. Samples were reacted with primary antibodies, 1:100 anti-CD31 (rat monoclonal IgG, ab7388, Abcam, Cambridge, UK), 1:100 anti-PDGFRβ (rabbit monoclonal IgG, C82A3, Cell Signaling, Danvers, MA), 1:100 anti-Ninj1 (rabbit polyclonal IgG, ab213695, Abcam). Immunoreactions were detected using Alexa fluor 488 and Alexa Fluor 594 secondary antibodies (goat anti-rat IgG, A11006 and A11037, Life Technologies, Waltham, MA) and -Alexa Fluor 647 (goat anti-rabbit IgG, A21244, Invitrogen). To observe vascular remodeling including intimal hyperplasia and adventitial microvessels, tissue was cleared to transparency using RapiClear 1.47 (RC147001, SunJin Lab, Hsinchu, Taiwan). Clarified vessels were imaged using a confocal fluorescence microscope (FV1000D, Olympus, Tokyo, Japan) and 20-30 serial slides (40x) in 10-μm steps were z-stacked and projected in a three-dimensional view before further quantitative analyses.

To estimate adventitial microvessel formation, three observation points were randomly selected for each sample and quantification was performed using image J (angiogenesis analyses). Total microvessel length was measured by manual tracing and stratified into three groups by microvessel diameter as follows; <4 μm, 4-8 μm, and >8 μm. Vessel length density (VLD) was measured as a ratio of microvessel length to total observation volume as well as occupation in length of stratified capillary diameter to total

vessel length. The number of microvasculature branching points was counted in observation volume and the number of pericytes that adhered to the observed microvessels (pericytes coverage) was counted.

To estimate vascular remodeling, a long axis view of the vessel was taken from 3D imaging data, and the areas of intimal and medial layers and total vessel area were measured using ImageJ software (Supplemental Fig. 1). Degree of intimal hyperplasia was evaluated as intimal-medial ratio and stenosis ratio as described previously(15, 38).

***In vitro* proliferation assay.** PCs were prepared, and Ninj1 expression in PCs were knocked down (Ninj1 KD) using Ninj1-specific siRNA as described previously(20). PCs treated with its scramble siRNA were used as control. Proliferation assay of PCs was performed using Premix WST-1 Cell Proliferation Assay System (MK400, Takara).

For estimation of proliferation of vascular smooth muscle cells (VSMCs), medial explants were prepared from thoracic aorta of NG2-CreER/*Ninj1*^{loxp} mice. The explants were incubated in Dulbecco's Modified Eagle Medium (DMEM) containing 20% fetal bovine serum (FBS) with or without 2 nM 4-hydroxytamoxifen (H7904, Sigma-Aldrich). After 7 days-incubation, $NG2^+$ cells were immunostained using 1:100 anti-NG2 antibody (rat monoclonal antibody, MABS1949-100UG, Merck, CA). The number of cells (either $NG2^+$ and $NG2^-$ VSMCs) sprouting/growing from explants was counted.

Reverse-transcriptase quantitative polymerase chain reaction (qPCR) analysis. Femoral arteries were freshly isolated, and dissolved in Trizol reagent (15596018, Life Technologies). RNA was purified from tissues using the RNeasy Mini Kit (74106, Qiagen, Venlo,), followed cDNA generation using iScript Reverse Transcription Supermix for reverse transcriptase (RT)-qPCR (1708840, Bio-Rad, Hercules, CA). RT-qPCR was performed with the following primers: glyceraldehyde-3-phosphate dehydrogenase (Gapdh, Mm99999915, Thermo Fisher Scientific), chondroitin sulfate proteoglycan 4

(Cspg4 (NG2), Mm00507257, Thermo Fisher Scientific), and Ninjurin-1 (Ninj1, Mm00479014, Thermo Fisher Scientific).

Gene microarray analysis. Femoral arteries were freshly isolated and stored at -80 ℃ until use. RNA was extracted from tissues as described above, and applied to microarray analysis using the three-dimensional (3D) Gene Mouse miRNA Oligo chip 24k (Toray Industries Inc., Tokyo, Japan) as described previously (13, 38). Intensity values greater than 2 standard deviations above the background signal were considered valid. The signal corresponding to each gene was normalized using the global normalization method (Cy3/Cy5 ratio median=1). Differential gene screening conditions were set as a fold change >2. Gene ontology (GO) analysis was performed to determine the roles of the differentially expressed mRNAs (DEmRNAs). Among 521 expressed genes related to inflammatory responses defined by GO analysis (biological process, item number 0006954), clustering analysis was performed using microarray gene expression in control and Ninj1 KO mice.

Statistical analysis. Normally distributed data and homogeneity of variance were confirmed using the F-test and Bartlett's test, respectively. A Student's t-test was used to compare two-groups. To compare three groups, one-way analysis of variance was used for data with a normal distribution, followed by Tukey's test. A P value of <0.05 was considered statistically significant.

Results

Vascular injury induces adventitial neovascularization and Ninjurin-1 expression.

Using transparent tissue samples, mouse femoral vessels were observed in a 3D view from adventitia to media to intima (Supplemental Fig. 1). In particular, formation of adventitial microvessels at the injured vasculature can be observed in detail. In a steady condition (sham group), adventitial microvessels were only slightly detected (Fig. 1A). In response to coiled wire-induced vascular injury, neovascularization in the adventitial layers was significantly enhanced (Figs. 1A, B). There was no significant difference in total length of microvessels on adventitia in NG2-CreER/*Ninj1*^{loxp} mice and their controls (Fig. 1B).

Ninjurin-1 expression is induced in response to tissue damage, such as ischemia and inflammation (2, 20, 36). Expression of *Ninj1* in whole femoral arteries was significantly increased in response to vascular injury and peaked at 1 week of vascular injury, and gradually decreased (Fig. 1C). Cells expressing NG2, a marker for pericytes and certain types of VSMCs in vessels(9), were observed at peri-vascular sites and medial VSMCs of non-injured vessels (Fig. 1D and Supplemental Fig. 2A). In response to vascular injury, NG2^{+}pericytes increased in parallel with enhanced adventitial neovascularization. At 1 week of vascular injury, Ninj1 expression was mostly observed in NG2^{+}PCs (Fig. 1D, supplemental Fig. 2A) and F4/80^{+} macrophages (Fig. 5A). Ninj1 expression was observed in medial VSMCs of non-injured vessels, but not detected in VSMCs in intimal layers of injured vascular walls (Fig. 1D). Therefore, enhanced Ninj1 expression in response to vascular injury would be due to the Ninj1 expression in adventitial cells.

Premature adventitial microvessels in mice with pericyte-specific deletion of Ninjurin-1.

Before vascular injury, *Ninj1* was selectively deleted in pericytes by treating NG2-CreER/*Ninj1*^{loxP} mice with tamoxifen (*Ninj1* KO)(20, 36). We have confirmed that expression of Ninj1 was specifically deleted in NG2^{+} cells but not in NG2^{-} cells of tamoxifen-treated NG2-CreER/*Ninj1*^{loxP} mice, although expression level of Ninj1 in whole femoral vessels was not altered (20). In Ninj1 KO mice, Ninj1 expression was not observe in adventitial pericytes but detected in macrophage in adventitia of injured vascular walls (Supplemental Fig. 2 and Fig. 5A). These data indicate that Nin1 expression was selectively decreased in NG2^{+}cells using NG2-CreER/*Ninj1*^{loxP} mice. Appropriate control groups in which Ninj1 expression was maintained were prepared as described in Methods. Four weeks after vascular injury, adventitial microvessel formation was evaluated (Fig. 2A).

Microvessel length in the adventitial layer tends to be increased but was not significantly difference between *Ninj1* KO mice and control mice (Fig. 2B). However, the length and proportion of smaller microvessls (diameter < 4 μm) were significantly increased in *Ninj1* KO mice compared with control mice (Figs. 2C). The number of vascular branches in adventitial microvessels, which represents vascular immaturity, was significantly higher in *Ninj1* KO mice (Fig. 2D). The number of pericytes associated with microvessels was not significantly different between *Ninj1* KO mice and control mice (Fig. 2E).

Pericyte-specific Ninj1 KO increases vascular permeability in adventitial microvessels.

Consist with previous study using the hind limb ischemia model (20), morphological data suggests that Ninjurin-1 in pericytes plays a critical role in the maturation of microvessels in the adventitia of injured vessels. To examine whether pericytes-specific deletion of Ninj1 induces functional fragility in adventitial microvessels, blood circulating vessels were stained by intravenous perfusion of FITC-labeled lectin. Similar to CD31-immunostained vessels, lectin-stained microvessels were observed at adventitial layers of injured vessels (Fig. 3A). Extravasated lectin spread over the microvessels, which manifested as patchy stained area in adventitial microvessels of injured arteries. However, the area of extravasation was significantly increased in *Ninj1* KO (Figs. 3A, B), suggesting that microvessels permeability is enhanced with pericytes-specific deletion of *Ninj1*.

To identify leakage of larger molecules from microvessels, FITC-labeled dextran (70 kDa) was perfused intravenously. Extravasation of FITC-labeled dextran at adventitial microvessels was observed, especially in *Ninj1* KO (Figs. 3A, C). In sham-operated non-injured arteries, no leaking microvessels were observed in either control groups or *Ninj1* KO mice (Figs. 3B, C).

Pericyte-specific Ninj1 KO enhances intimal hyperplasia in injured vasculature.

In response to wire-mediated intimal injury, neointimal formation is occurred, and terminated by reendothelialization within 3-4 weeks of vascular injury (15, 38). In a 3D-view of transparent tissues, vascular remodeling, including intimal hyperplasia was clearly observed in whole injured vascular walls (Supplemental Fig. 1). In the present study, injured intima was completely covered by an endothelial layer and intimal

hyperplasia terminated at 4 weeks in both control mice and *Ninj1* KO mice (Fig. 4A). The degree of intimal hyperplasia, estimated by the intimal-medial ratio, and stenosis ratio were significantly increased in *Ninj1* KO mice compared with controls (Figs. 4B, C). The medial layer and vascular lumen were not significantly different among these groups (Supplemental Fig.3).

$NG2^{+}$VSMCs were observed in medial layers, and Ninj1 was expressed in these cells (Fig.1). Thus, to test the effect of Ninj1 on proliferation of medial $NG2^{+}$VSMCs using vascular medial explants of NG2-CreER/*Ninj1*^{loxP} mice. Deletion of Ninj1 gene in medial explants was induced by treatment with hydroxy-tamoxifen. There were no differences in numbers of sprouting and proliferating VSMCs between Ninj1 KO and control groups (Fig. 4D). More importantly, the ratio of $NG2^{+}$cells in proliferating VSMCs were relatively low (~10%) and not difference in Ninj1 KO and control groups (Fig. 4D).

Four weeks after vascular injury, a microarray gene analysis of the femoral arteries demonstrated that the marker gene expression in endothelial cells, pericytes, and vascular SMCs was similar between *Ninj1* KO mice and control mice (Table 1). However, in particular, expression of α-smooth muscle actin (αSMA) and smooth muscle 22α (SM22 α), markers of differentiated vascular SMCs (1), was low in *Ninj1* KO mice (Table 1).

Persistent adventitial inflammation in pericyte-specific Ninj1 KO mice.

In atherosclerotic lesions, increased permeability in fragile vasa vasorum enables entry of blood components, including inflammatory cells and red blood cells, into vascular walls (33, 37). The number of macrophages in the vascular walls, especially in the adventitial layer was significantly increased in *Ninj1* KO mice compared with control mice (Figs. 5A-C).

Consistent with this finding, the gene expression profile of injured vessels showed that inflammatory status was increased in *Ninj1* KO mice compared with control mice (Table 2). Among 521 expressed genes related to inflammatory responses defined by GO analysis (biological process, item number 0006954), most of genes were upregulated (Fig.5C), e.g. the number of upregulated and downregulated DEmRNAs were 69 and 1, respectively. The upregulated genes include interleukin (IL)1β, chemokines, and inflammatory cells-related genes such as CD74, chemokine receptors (CCR) and allograft inflammatory factor-1 (AIF1)(22, 35) (Table 2).

Discussion

A relationship between abnormal vasa vasorum formation, including enhanced growth and immaturation, and vascular remodeling has been demonstrated using clinical samples and animal models of atherosclerosis (6, 26, 31). However, this new pathological concept, specifically the outside-in theory has arisen mostly due to indirect correlative evidence. In addition, it is difficult to estimate microvessel formation and vascular remodeling using conventional histological analyses, such as thin-slice view. The vasa vasorum is distributed over vascular walls in complex mesh-like pattern, and the degree of vascular remodeling, including vascular wall thickening, varies between sites. These technical limitations have made it difficult to clarify the role of the vasa vasorum in pathophysiological vascular remodeling, such as atherosclerosis. In the present study, 3D-imaging of transparent tissues clearly showed abnormalities in newly formed adventitial microvesssels, both quantitatively and qualitatively. We observed that pericytes-specific *Ninj1* deletion inhibits vascular maturation of adventitial microvasculature in response to vascular injury and exacerbates vascular remodeling (Supplemental Fig. 5).

In early phase of angiogenesis, EC tubes are sprouted from pre-existed vessels, then vascular maturation starts by association of PCs to EC-tubes(3, 11). Ninj1 which is expressed in response to angiogenic stimuli, such 326 as inflammation, acts on this early step of vascular maturation(19, 20). Ninj1 does not affect pre-existing mature microvessels(20). Matured vessels are maintained by other factors such as PDGF and angiopoietin, after Ninj1 expression is decreased to basal level. When expression of Ninj1 at one week after vascular remodeling is inhibited, adventitial neovessels does not mature appropriately and microvasculature grown in adventitia was impaired morphologically and functionally during vascular remodeling (Fig. 2, 3). Intraplaque microbleeding is a crucial event for infiltration of inflammatory cells and subsequent chronic inflammation

in atherosclerotic lesion(6, 33). Intraplaque microbleeding is thought to originate from defective formation of the vasa vasorum, including hyper-permeability(31). Therefore, we thought that fragile microvasculature may induce microbleeding, that is one of mechanisms for accumulation of macrophage and prolonged inflammation in adventitia (Fig. 5).

Ninj1 KO in pericytes enhanced the expression of angiogenic factors(20)and inflammatory cytokines (Supplemental table) and these paracrine effects also might contribute to enhanced inflammation (Fig. 5D, Table 2). Recently, it is reported that the interaction of macrophage and PCs contributes to tissue regeneration and remodeling(21, 32). PC mediates the activation of macrophage through paracrine effects(32). Recently, soluble Ninjurin1 derived from extracellular portion of Ninjurin1 of affect the function of macrophage to attenuate the process of atherosclerosis(12). Thus, alternatively, we proposed that deletion of Ninj1 in PCs may also affect the function of macrophage and contribute to the prolonged inflammation, resulting in deteriorated vascular remodeling.

Pericytes-specific *Ninj1* deletion significantly enhanced intimal hyperplasia (Fig. 4). *Ninj1* KO did not affect intimal restoration, because intimal damage was completely restored 4 weeks after vascular injury by reendothelialization in both *Ninj1* KO mice and control mice (Fig. 4). While intimal injury was restored equally, adventitial inflammation was enhanced in *Ninj1* KO mice. Features of activation/dedifferentiation of VSMCs by certain stimuli, such as inflammatory cytokines, coincide with enhanced growth and decreased expression of αSMA(7, 8). In line with speculation that enhanced intimal hyperplasia is due to excess growth of VSMCs, marker gene expression for their contractile non-proliferative phenotype such as αSMA and Tagln(1) was decreased in injured vascular walls of *Ninj1* KO mice (Table 1). In addition to $NG2^+$pericytes in adventitial area, some of VSMCs are detected as $NG2^+$cells in medial layer of non-injured

vessels. $NG2^+$cells in hyperplastic intimal layer were observed, but their ratio among intimal cells was relatively low (Fig. 1D). Ninj1 deletion in $NG2^+$VSMCs did not affect proliferation of VSMCs, not only $NG2^+$cells but also other VSMCs (Fig. 4D). Therefore, contribution of Ninj1 to the function of $NG2^+$VSMCs as regards the vascular remodeling might be low.

Pericyte coverage is one of the morphological features of vascular maturation, andits level was significantly attenuated in ischemic skeletal muscles of *Ninj1* KO mice(20). However, pericyte coverage was not significantly different between control mice and *Ninj1*KO mice in this study (Fig. 2E). In particular, compared with skeletal muscle tissues, the formation and distribution of the microvasculature was somewhat complexed in loose adventitial tissues, which comprise fibrous components. Thus, estimation of pericyte coverage in adventitial microvessels is technically difficult, even though observation is performed using 3D-imaging. Expression of PDGFRβ in pericytes is altered by pathophysiological conditions such as angiogenesis and inflammation(30, 41). At 4 weeks after vascular injury, expression level of PDGFRβ in pericytes would be decreased in control, in which vascular remodeling is terminated. Thus, we thought that $PDGFR\beta^+$ pericytes might be under estimated in control, while expression level of PDGFRβ in pericytes is still upregulated in *Ninj1* KO mice. Immunostaining of pericytes in transparent tissues can be done with only anti-PDGFRβ antibody in our hands so far. Alternatively, Ninjurin-1 exerts paracrine effects that mediate vascular maturation, *e.g.* Ninjurin-1 increases the production of angiopoietin 1(20), which influences vascular maturation and stabilization(16).

Vascular maturation is closely related to nerve reinnervation of the vasculature(25, 28). Vascular stability and maturation of adventitial microvessels grown in response to vascular injury are regulated by perivascular nerve regeneration(4). We reported that $EphA7^+$ multipotent pericytes, which differentiate into Schwann cells, may play an

important role in regeneration of peripheral nerve along with angiogenesis(36). Ninjurin-1 in EphA7+ pericytes is crucial for neurogenesis potency, and peripheral nerve regeneration/repair from sciatic nerve injury is reduced in pericyte-specific *Ninj1* KO mice. Thus, it is postulated that Ninjurin-1 contributes to microvascular maturation of the vasa vasorum through peripheral nerve regeneration. To test this hypothesis and estimate the morphological features of the microvasculature and peripheral nerves in detail, development of a method to observe the vasculature and nerve in 3D with a higher image resolution is required.

Jeon *et al* reported that soluble form of Ninj1 (sNinj1) cleaved from Ninj1 on macrophage attenuated the activity of inflammatory cells and inhibited atherosclerosis(12). *Ninj1* KO in bone marrow exacerbated atherosclerosis because of the lack of sNinj1 released from macrophage. In the present study, we confirmed that Ninj1 was expressed in adventitial F4/80+macrophage accumulated in response to vascular injury and their expression level in macrophage was not affected in NG2-CreER/Ninj1loxP mice (Fig. 5). The cellular mechanism of anti-398 inflammatory effect of sNinj1 is still unclear. It is interesting to test whether sNinj1 affects Ninj1 molecule expressed on cellular surface of macrophage and/or other cell types including pericytes.

Based on the outside-in concept, inhibitions of plaque angiogenesis has been proposed for anti-atherosclerotic therapy for plaque stabilization and further regression (6, 31). Several investigations using animal models have demonstrated that inhibition of neovascularization can dampen the expansion of vasa vasorum neovessel formation and attenuate atherosclerotic lesion progression (10, 23, 24). However, it should be noted that vasa vasorum growth is a compensatory response to vascular remodeling, including plaque formation and intimal hyperplasia. Therefore, mere anti-angiogenic therapies may induce further ischemia and inflammation within vascular walls. Furthermore, it is well

known that anti-angiogenic therapies often have transient or limited clinical success due to inherent or compensatory resistance mechanisms in cancer therapy (5). Intraplaque hemorrhage is a crucial event for persistent chronic inflammation and subsequent plaque progression and vulnerability in clinical atherosclerotic lesion. Intraplaque hemorrhage is thought to originate from defective formation of the vasa vasorum, including hyper-permeability (6, 31, 33). Thus, vascular maturation as opposed to mere anti-angiogenic therapy may be an alternative strategy for a long-term therapeutic effect, and interesting targets to restore vascular integrity include orchestrators of angiogenesis and vascular maturation.

The present study demonstrated that 3D imaging analysis of transparent arteries is a useful tool to estimate of vascular remodeling and vasa vasorum growth, and that Ninjurin-1 is a crucial molecule for pericytes to form mature vasa vasorum and regulate vascular inflammation and remodeling in injured vasculature (Supplemental Fig. 3). The study, which use a unique pericyte-specific *Ninj1* KO mouse model, supports the notion that the adventitial environment contributes to vascular remodeling. Regulation of adventitial inflammation via stable and mature of adventitial microvessels may be an effective strategy to prevent atherosclerosis. Ninjurin-1 is an attractive target to normalize microvessels for anti-atherosclerotic therapy.

Acknowledgments

K.H. performed cell biology and animal experiments and data analyses, data interpretation, and manuscript writing. K.K., A.M., T.H., A.Y. and T.T. performed cell biology and animal experiments and analyzed data. N.N. and N.T. assisted with microarray analysis. M.K., R.M., and Y.M. helped with biochemical and histological analysis and discussion. N.H. supervised the research. J.K. performed conception and design, data interpretation, manuscript writing, final approval manuscript. We also thank S. Takahashi, K. Kanno, Y. Horikawa, M. Ishizaka, A. Oda for laboratory assistance.

Sources of Funding

This work was supported by JSPS KAKENHI grant number (17H04170, 17K19368 to J.K.).

Disclosures

None declared

References

1. Allahverdian S, Chaabane C, Boukais K, Francis GA, and Bochaton-Piallat ML. Smooth muscle cell fate and plasticity in atherosclerosis. Cardiovascular research 114:393 540-550, 2018.
2. Araki T, and Milbrandt J. Ninjurin, a novel adhesion molecule, is induced by nerve injury and promotes axonal growth. Neuron 17: 353-361, 1996.
3. Armulik A, Genove G, and Betsholtz C. Pericytes: developmental, physiological, and pathological perspectives, problems, and promises. Developmental cell 21: 193-215, 2011.
4. Asanome A, Kawabe J, Matsuki M, Kabara M, Hira Y, Bochimoto H, Yamauchi A, Aonuma T, Takehara N, Watanabe T, and Hasebe N. Nerve growth factor stimulates regeneration of perivascular nerve, and induces the maturation of microvessels around the injured artery. Biochemical and biophysical research communications 443: 150-155, 2014.
5. Bergers G, and Hanahan D. Modes of resistance to anti-angiogenic therapy. Nature reviews Cancer 8: 592-603, 2008.
6. Boyle EC, Sedding DG, and Haverich A. Targeting vasa vasorum dysfunction to prevent atherosclerosis. Vascular pharmacology 96-98: 5-10, 2017.
7. Campbell JH, Kocher O, Skalli O, Gabbiani G, and Campbell GR. Cytodifferentiation and expression of alpha-smooth muscle actin mRNA and protein during primary culture of aortic smooth muscle cells. Correlation with cell density and proliferative state. Arteriosclerosis 9: 633-643, 1989.
8. Chen L, DeWispelaere A, Dastvan F, Osborne WR, Blechner C, Windhorst S, and Daum G. Smooth Muscle-Alpha Actin Inhibits Vascular Smooth Muscle Cell

Proliferation and Migration by Inhibiting Rac1 Activity. PloS one 11: e0155726, 2016.

9. Diaz-Flores L, Gutierrez R, Madrid JF, Varela H, Valladares F, Acosta E, Martin-Vasallo P, and Diaz-Flores L, Jr. Pericytes. Morphofunction, interactions and pathology in a quiescent and activated mesenchymal cell niche. Histology and histopathology 24: 909-969, 2009.
10. Drinane M, Mollmark J, Zagorchev L, Moodie K, Sun B, Hall A, Shipman S, Morganelli P, Simons M, and Mulligan-Kehoe MJ. The antiangiogenic activity of rPAI-1(23) inhibits vasa vasorum and growth of atherosclerotic plaque. Circulation research 104: 337-345, 2009.
11. Gaengel K, Genove G, Armulik A, and Betsho 426 ltz C. Endothelial-mural cell signaling in vascular development and angiogenesis. Arteriosclerosis, thrombosis, and vascular biology 29: 630-638, 2009.
12. Jeon S, Kim TK, Jeong SJ, Jung IH, Kim N, Lee MN, Sonn SK, Seo S, Jin J, Kweon HY, Kim S, Shim D, Park YM, Lee SH, Kim KW, Cybulsky MI, Shim H, Roh TY, Park WY, Lee HO, Choi JH, Park SH, and Oh GT. Anti-Inflammatory Actions of Soluble Ninjurin-1 Ameliorate Atherosclerosis. Circulation 142: 1736-1751, 2020.
13. Kabara M, Kawabe J, Matsuki M, Hira Y, Minoshima A, Shimamura K, Yamauchi A, Aonuma T, Nishimura M, Saito Y, Takehara N, and Hasebe N. Immortalized multipotent pericytes derived from the vasa vasorum in the injured vasculature. A cellular tool for studies of vascular remodeling and regeneration. Laboratory investigation; a journal of technical methods and pathology 94: 1340-1354, 2014.
14. Kawabe J, and Hasebe N. Role of the vasa vasorum and vascular resident stem cells in atherosclerosis. BioMed research international 2014: 701571, 2014.

15. Kawabe J, Yuhki K, Okada M, Kanno T, Yamauchi A, Tashiro N, Sasaki T, Okumura S, Nakagawa N, Aburakawa Y, Takehara N, Fujino T, Hasebe N, Narumiya S, and Ushikubi F. Prostaglandin I2 promotes recruitment of endothelial progenitor cells and limits vascular remodeling. Arteriosclerosis, thrombosis, and vascular biology 30: 464-470, 2010.
16. Koh GY. Orchestral actions of angiopoietin-1 in vascular regeneration. Trends Mol Med 19: 31-39, 2013.
17. Lee HJ, Ahn BJ, Shin MW, Jeong JW, Kim JH, and Kim KW. Ninjurin1 mediates macrophage-induced programmed cell death during early ocular development. Cell death and differentiation 16: 1395-1407, 2009.
18. Maiellaro K, and Taylor WR. The role of the adventitia in vascular inflammation. Cardiovascular research 75: 640-648, 2007.
19. Matsuki M, Kabara M, Saito Y, Shimamura K, Minoshima A, Nishimura M, Aonuma T, Takehara N, Hasebe N, and Kawabe J. Ninjurin1 is a novel factor to regulate angiogenesis through the function of pericytes. Circulation journal: official journal of the Japanese Circulation Society 79: 1363-1371, 2015.
20. Minoshima A, Kabara M, Matsuki M, Yoshida Y, Kano K, Tomita Y, Hayasaka T, Horiuchi K, Saito Y, Aonuma T, Nishimura M, Maruyama K, Nakagawa N, Sawada J, Takehara N, Hasebe N, and Kawabe JI. Pericyte-Specific Ninjurin1 Deletion Attenuates Vessel Maturation and Blood Flow Recovery in Hind Limb Ischemia. Arteriosclerosis, thrombosis, and vascular biology 38: 2358-2370, 2018.
21. Minutti CM, Modak RV, Macdonald F, Li F, Smyth DJ, Dorward DA, Blair N, Husovsky C, Muir A, Giampazolias E, Dobie R, Maizels RM, Kendall TJ, Griggs DW, Kopf M, Henderson NC, and Zaiss DM. A Macrophage-Pericyte Axis Directs

Tissue Restoration via Amphiregulin-Induced Transforming Growth Factor Beta Activation. Immunity 50: 645-654 e646, 2019.

22. Mishima T, Iwabuchi K, Fujii S, Tanaka SY, Ogura H, Watano-Miyata K, Ishimori N, Andoh Y, Nakai Y, Iwabuchi C, Ato M, Kitabatake A, Tsutsui H, and Onoe K. Allograft inflammatory factor-1 augments macrophage phagocytotic activity and accelerates the progression of atherosclerosis in ApoE-/- mice. International journal of molecular medicine 21: 181-187, 2008.
23. Mollmark J, Ravi S, Sun B, Shipman S, Buitendijk M, Simons M, and Mulligan-Kehoe MJ. Antiangiogenic activity of rPAI-1(23) promotes vasa vasorum regression in hypercholesterolemic mice through a plasmin-dependent mechanism. Circulation research 108: 1419-1428, 2011.
24. Moulton KS, Vakili K, Zurakowski D, Soliman M, Butterfield C, Sylvin E, Lo KM, Gillies S, Javaherian K, and Folkman J. Inhibition of plaque neovascularization reduces macrophage accumulation and progression of advanced atherosclerosis. Proceedings of the National Academy of Sciences of the United States of America 100: 4736-4741, 2003.
25. Mukouyama YS, Gerber HP, Ferrara N, Gu C, and Anderson DJ. Peripheral nerve-derived VEGF promotes arterial differentiation via neuropilin 1-mediated positive feedback. Development 132: 941-952, 2005.
26. Mulligan-Kehoe MJ, and Simons M. Vasa vasorum in normal and diseased arteries. Circulation 129: 2557-2566, 2014.
27. Odoardi F, Sie C, Streyl K, Ulaganathan VK, Schlager C, Lodygin D, Heckelsmiller K, Nietfeld W, Ellwart J, Klinkert WE, Lottaz C, Nosov M, Brinkmann V, Spang R, Lehrach H, Vingron M, Wekerle H, Flugel-Koch C, and Flugel A. T cells become licensed in the lung to enter the central nervous system. Nature 488: 675-679, 2012.

28. Pardanaud L, Pibouin-Fragner L, Dubrac A, Mathivet T, English I, Brunet I, Simons M, and Eichmann A. Sympathetic Innervation Promotes Arterial Fate by Enhancing Endothelial ERK Activity. Circulation research 119: 607-620, 2016.
29. Rademakers T, Douma K, Hackeng TM, Post MJ, Sluimer JC, Daemen MJ, Biessen EA, Heeneman S, and van Zandvoort MA. Plaque-associated vasa vasorum in aged apolipoprotein E-deficient mice exhibit proatherogenic functional features in vivo. Arteriosclerosis, thrombosis, and vascular biology 33: 249-256, 2013.
30. Raica M, and Cimpean AM. Platelet-Derived Growth Factor (PDGF)/PDGF Receptors (PDGFR) Axis as Target for Antitumor and Antiangiogenic Therapy. Pharmaceuticals (Basel) 3: 572-599, 2010.
31. Sedding DG, Boyle EC, Demandt JAF, Sluimer JC, Dutzmann J, Haverich A, and Bauersachs J. Vasa Vasorum Angiogenesis: Key Player in the Initiation and Progression of Atherosclerosis and Potential Target for the Treatment of Cardiovascular Disease. Frontiers in immunology 9: 706, 2018.
32. Shibahara T, Ago T, Tachibana M, Nakamura K, Yamanaka K, Kuroda J, Wakisaka Y, and Kitazono T. Reciprocal Interaction Between Pericytes and Macrophage in Poststroke Tissue Repair and Functional Recovery. Stroke 51: 3095-3106, 2020.
33. Sluimer JC, Kolodgie FD, Bijnens AP, Maxfield K, Pacheco E, Kutys B, Duimel H, Frederik PM, van Hinsbergh VW, Virmani R, and Daemen MJ. Thin-walled microvessels in human coronary atherosclerotic plaques show incomplete endothelial junctions relevance of compromised structural integrity for intraplaque microvascular leakage. Journal of the American College of Cardiology 53: 1517-1527, 2009.

34. Stenmark KR, Yeager ME, El Kasmi KC, Nozik-Grayck E, Gerasimovskaya EV, Li M, Riddle SR, and Frid MG. The adventitia: essential regulator of vascular wall structure and function. Annual review of physiology 75: 23-47, 2013.
35. Tian Y, Kelemen SE, and Autieri MV. Inhibition of AIF-1 expression by constitutive siRNA expression reduces macrophage migration, proliferation, and signal transduction initiated by atherogenic stimuli. American journal of physiology Cell physiology 290: C1083-1091, 2006.
36. Tomita Y, Horiuchi K, Kano K, Tatsukawa T, Matsuo R, Hayasaka T, Yoshida Y, Kabara M, Yasuda S, Nakajima K, Nakagawa N, Takehara N, Okizaki A, Hasebe N, and Kawabe JI. Ninjurin 1 mediates peripheral nerve regeneration through Schwann cell maturation of NG2-positive cells. Biochemical and biophysical research communications 2019.
37. Virmani R, Kolodgie FD, Burke AP, Finn AV, Gold HK, Tulenko TN, Wrenn SP, and Narula J. Atherosclerotic plaque progression and vulnerability to rupture: angiogenesis as a source of intraplaque hemorrhage. Arteriosclerosis, thrombosis, and vascular biology 25: 2054-2061, 2005.
38. Yamauchi A, Kawabe J, Kabara M, Matsuki M, Asanome A, Aonuma T, Ohta H, Takehara N, Kitagawa T, and Hasebe N. Apurinic/apyrimidinic endonucelase 1 maintains adhesion of endothelial progenitor cells and reduces neointima formation. American journal of physiology Heart and circulatory physiology 305: H1158-1167, 2013.
39. Yin GN, Choi MJ, Kim WJ, Kwon MH, Song KM, Park JM, Das ND, Kwon KD, Batbold D, Oh GT, Koh GY, Kim KW, Ryu JK, and Suh JK. Inhibition of Ninjurin 1 restores erectile function through dual angiogenic and neurotrophic effects in the

diabetic mouse. Proceedings of the National Academy of Sciences of the United States of America 111: E2731-2740, 2014.

40. Yoshida Y, Kabara M, Kano K, Horiuchi K, Hayasaka T, Tomita Y, Takehara N, Minoshima A, Aonuma T, Maruyama K, Nakagawa N, Azuma N, Hasebe N, and Kawabe JI. Capillary-resident EphA7(+) pericytes are multipotent cells with anti-ischemic effects through capillary formation. Stem cells translational medicine 9: 120-130, 2020.
41. Zhang J, Cao R, Zhang Y, Jia T, Cao Y, and Wahlberg E. Differential roles of PDGFR-alpha and PDGFR-beta in angiogenesis and vessel stability. FASEB J 23: 153-163, 2009.

Figure 1

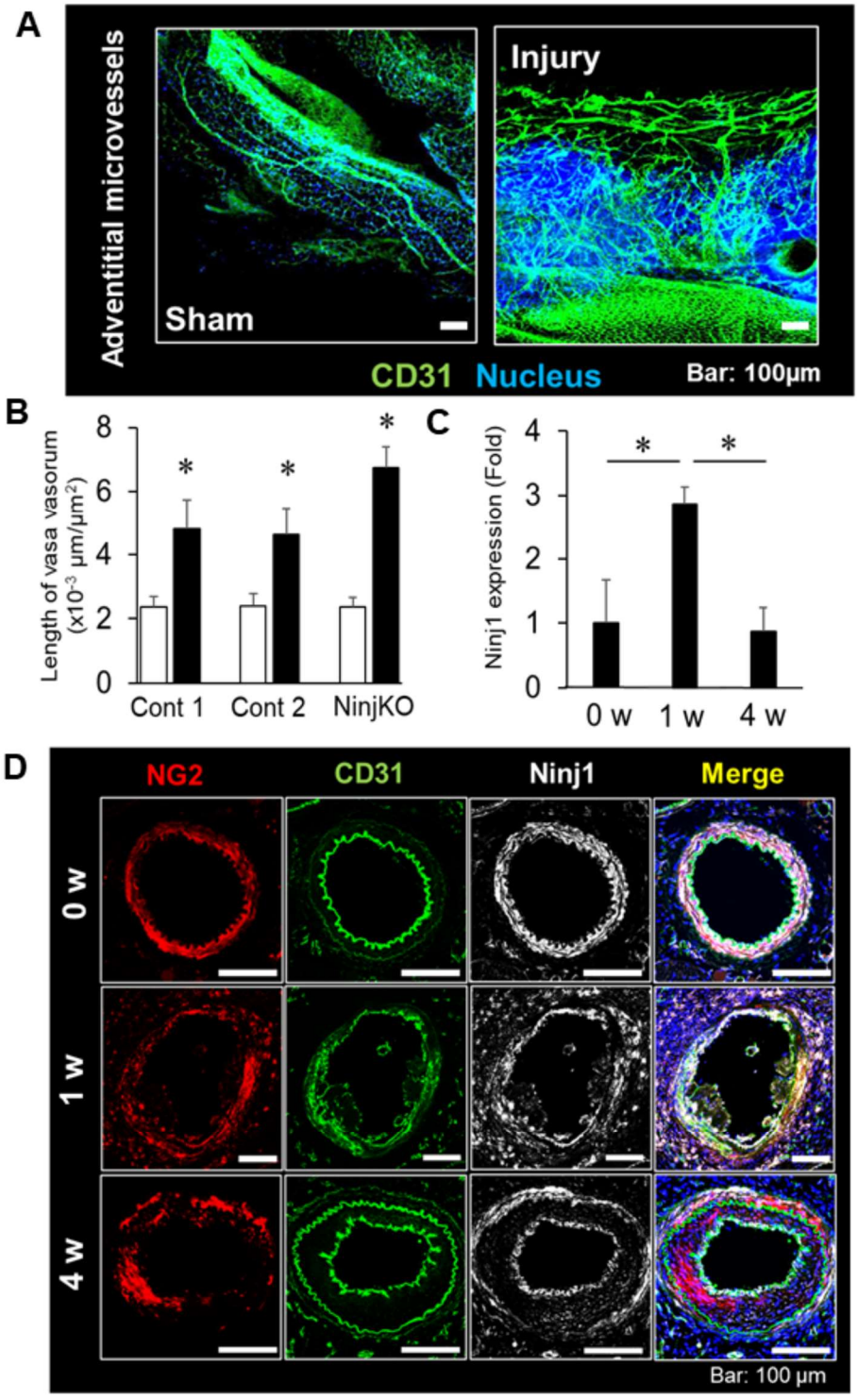
A
Adventitial microvessels
Sham
Injury
CD31 Nucleus
Bar: 100μm
B
Length of vasa vasorum (x10⁻³ μm/μm²)
0
2
4
6
8
*
*
*
Cont 1
Cont 2
NinjKO
C
Ninj1 expression (Fold)
0
1
2
3
4
*
*
0 w
1 w
4 w
D
NG2
CD31
Ninj1
Merge
0 w
1 w
4 w
Bar: 100 μm

Figure 1. Formation of adventitial microvessels and expression of Ninjurin-1 in response to vascular injury. A. Four weeks after vascular injury, the femoral arteries were fixed and treated for tissue transparency. CD31-immunostained microvessels in adventitial areas were observed three-dimensionally in wire-induced injury or sham-operated femoral arteries (sham). Nuclei were counterstained with Hoechst 33342. Serial confocal images were z-stacked and projected. **B.** The total microvessel length in observed adventitial areas was measured. NG2-CreER/Ninj1loxP mice were treated with tamoxifen to create pericyte-specific Ninj1 knockout mice (Ninj1 KO). Tamoxifen-treated NG2-CreER and vehicle-treated NG2-CreER/*Ninj1*^{loxP} mice were allocated to control groups 1 and 2, respectively. Open bars: sham, closed bars: Injury. **C.** Ninj1 expression in the arteries at indicated time after vascular injurywas estimated by reverse transcriptase quantitative PCR. **D.** Immunostaining view of pericytes (NG2), endothelial cells (CD31), and Ninjurin1 (Ninj1) in a short axis section of femoral arteries. Values are represented as the mean ± SEM. *$P<0.05$ compared with each open bar (n=7). Scale bars = 100 μm.

Figure 2

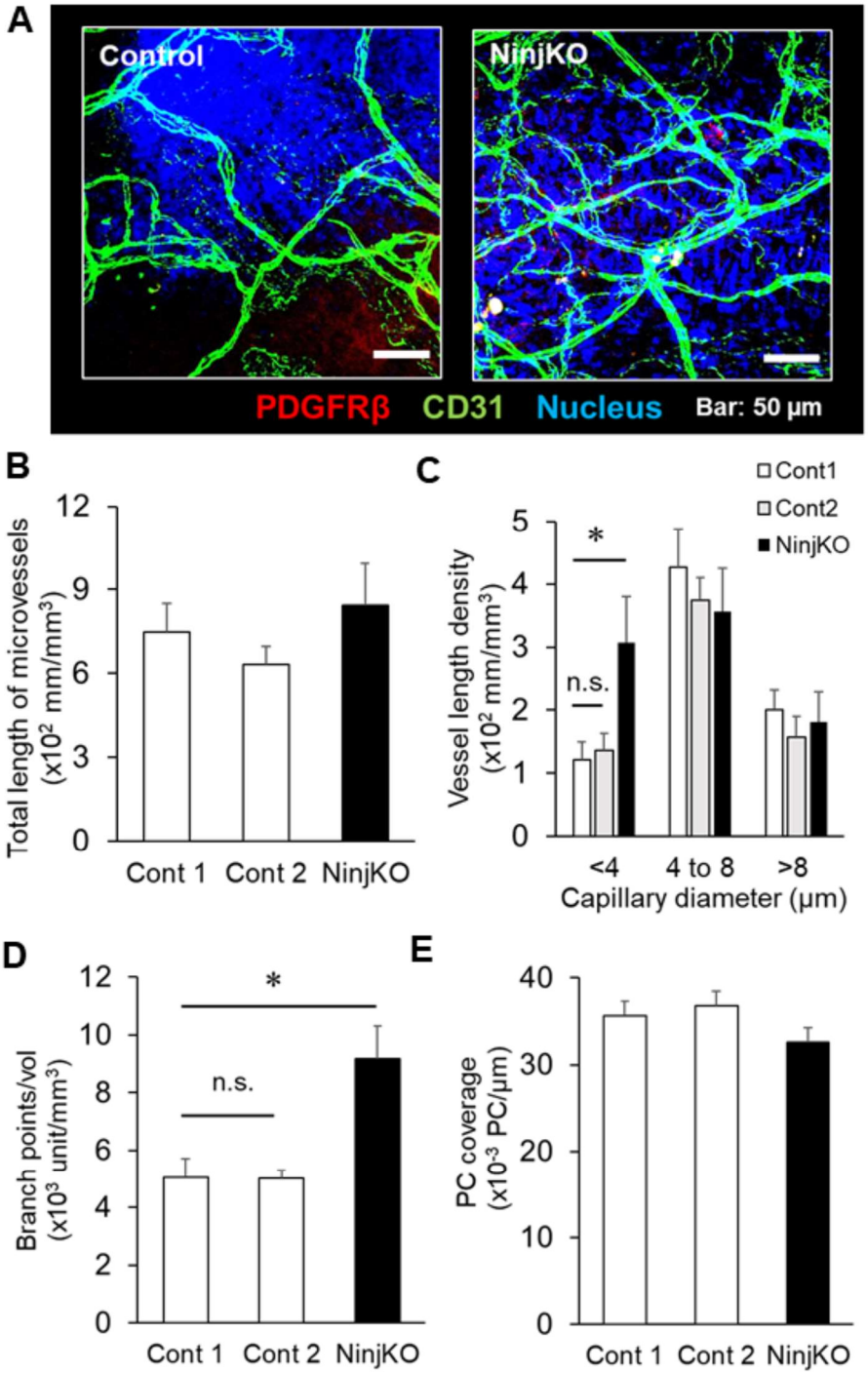
A
Control
NinjKO
PDGFRβ CD31 Nucleus Bar: 50 μm
B
Total length of microvessels (x10² mm/mm³)
0
3
6
9
12
Cont 1 Cont 2 NinjKO
C
Cont1
Cont2
NinjKO
Vessel length density (x10² mm/mm³)
0
1
2
3
4
5
*
n.s.
<4 4 to 8 >8
Capillary diameter (μm)
D
Branch points/vol (x10³ unit/mm³)
0
2
4
6
8
10
12
*
n.s.
Cont 1 Cont 2 NinjKO
E
PC coverage (x10⁻³ PC/μm)
0
10
20
30
40
Cont 1 Cont 2 NinjKO

Figure 2. Effects of Ninj1 deletion on formation of adventitial microvessels in injured vasculature. A. Microvessel formation in adventitial layers was observed three-dimensionally by immunostaining with $CD31^+$ endothelial tubes and $PDGFR\beta^+$ pericytes after 4 weeks of vascular injury of Ninj1 KO and control mice. Nuclei were counterstained with Hoechst 33342. **B-C.** The length of adventitial microvessels with different diameters were measured (<4 mm, 4-8 mm, > 8 mm). The total length and length of each stratified microvessels were calculated. **D, E.** The number of microvessel branches and the number of pericytes attached to microvessels were calculated. Values are presented as the mean ± SEM. *P<0.05, **P<0.01 (n=5-8). n.s.: not significant. Scale bars = 50 μm.

Figure 3

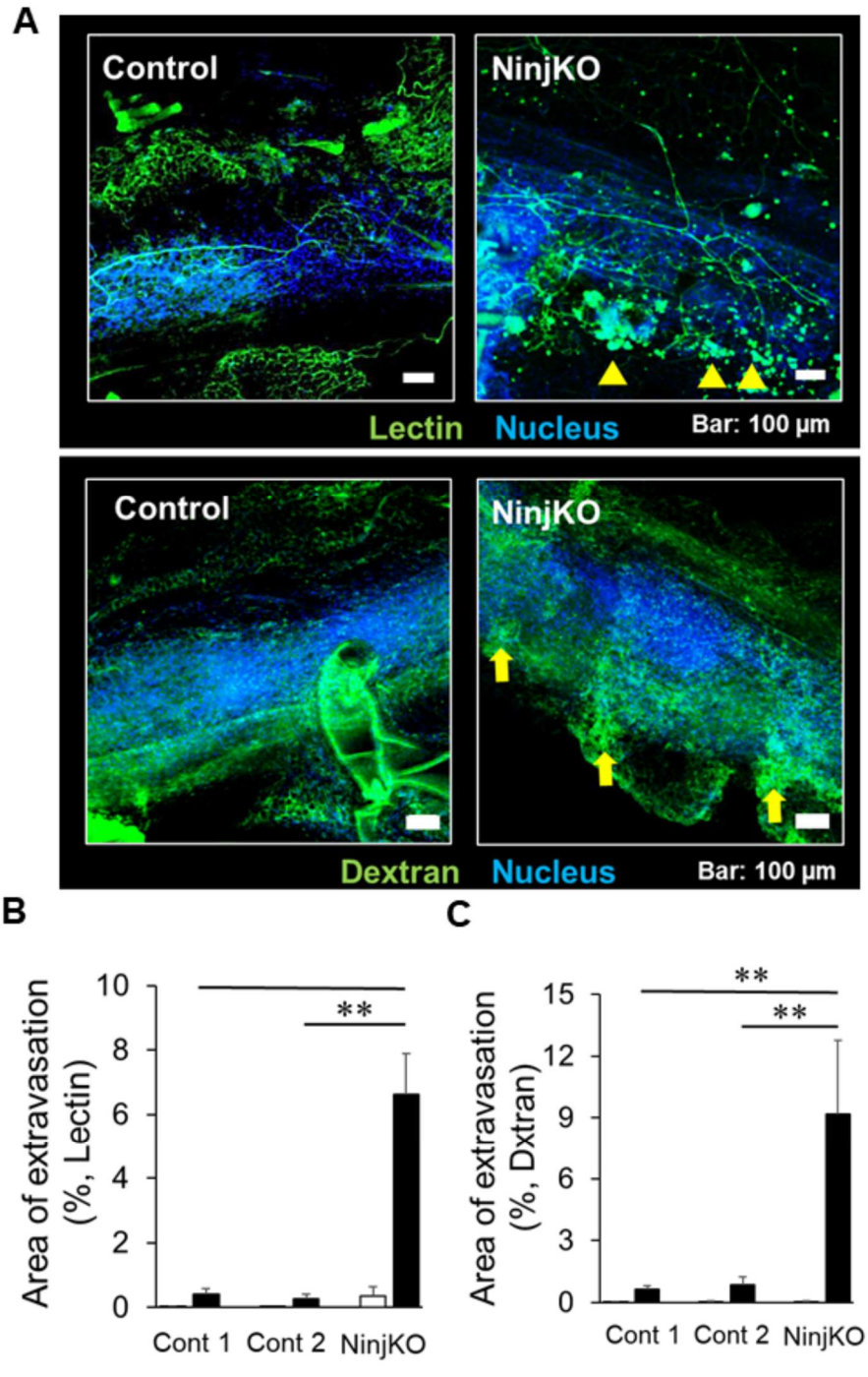
A
Control
NinjKO
Lectin
Nucleus
Bar: 100 μm
Control
NinjKO
Dextran
Nucleus
Bar: 100 μm
B
Area of extravasation (%, Lectin)
10
8
6
4
2
0
**
Cont 1
Cont 2
NinjKO
C
Area of extravasation (%, Dxtran)
15
12
9
6
3
0
**
**
Cont 1
Cont 2
NinjKO

Figure 3. Permeability of adventitial microvessels in injured vasculature. A. Circulating microvessels were stained by perfusing of FITC-labeled lectin or FITC-labeled-dextran (70 kDa) 4 weeks after arterial injury. In a three-dimensional view of the adventitial layer, fluorescent indicators leaked from microvessels. Leakage is observed as a patchy stained area (arrowhead). Nuclei were counterstained with Hoechst 33342. Scale bars = 100 μm. **B, C.** The extravasation area of FITC-labeled lectin and FITC-labeled dextran were measured and calculated as a ratio of fluorescent signal to total area. Open bars: sham operation; closed bars: injury. Values are presented as mean ± SEM. **P<0.01 (n=5-9).

Figure 4

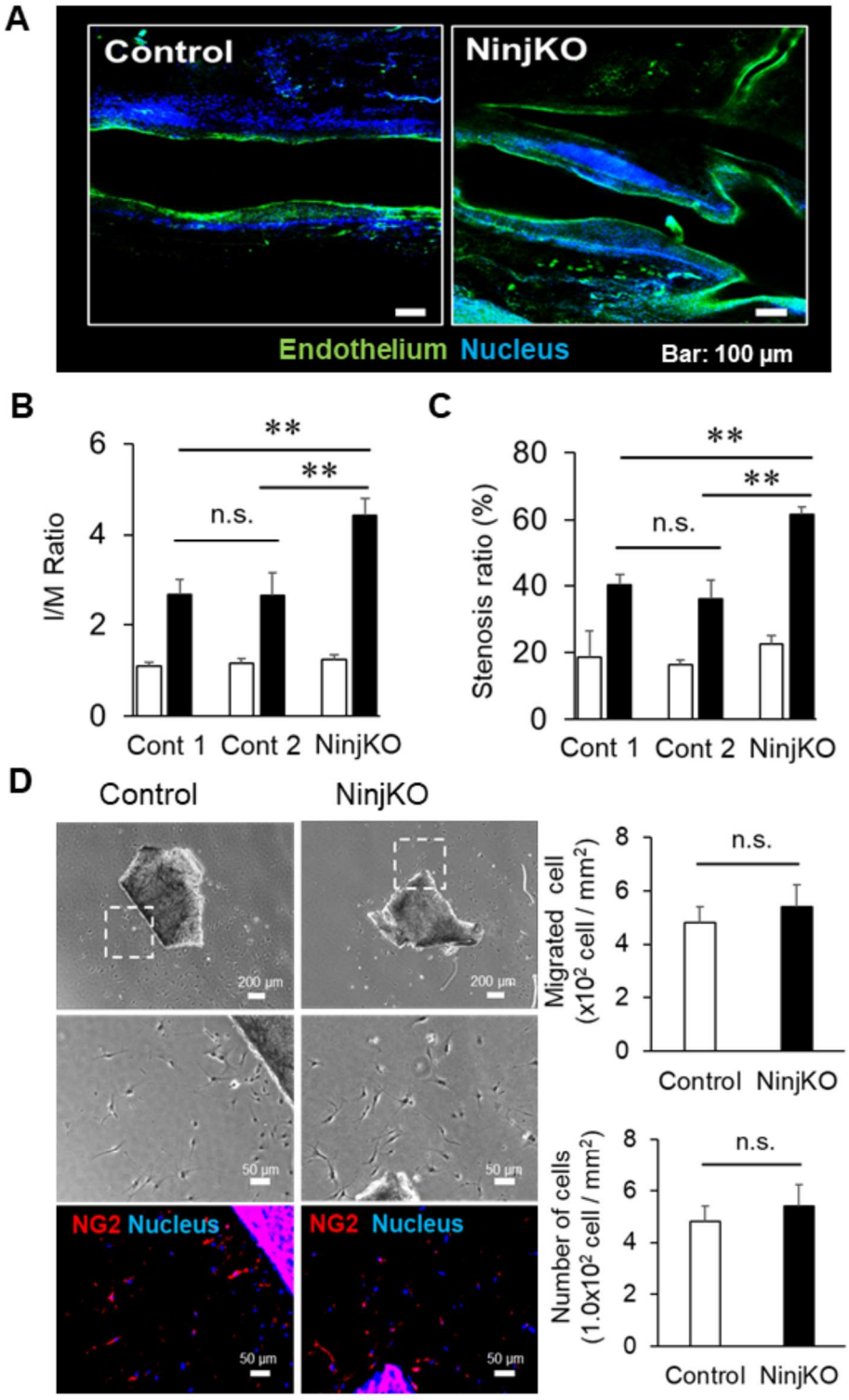
A
Control
NinjKO
Endothelium Nucleus
Bar: 100 μm
B
I/M Ratio
6
4
2
0
**
**
n.s.
Cont 1 Cont 2 NinjKO
C
Stenosis ratio (%)
80
60
40
20
0
**
**
n.s.
Cont 1 Cont 2 NinjKO
D
Control
NinjKO
200 μm
50 μm
NG2 Nucleus
Migrated cell (x10² cell / mm²)
8
6
4
2
0
n.s.
Control NinjKO
Number of cells (1.0x10² cell / mm²)
8
6
4
2
0
n.s.
Control NinjKO

Figure 4. Effects of Ninj1 KO on intimal hyperplasia in response to intimal injury.

A. The long axis view of three-dimensional femoral arteries was observed 4 weeks after vascular injury. The endothelial (intimal) layer was stained using FITC-labeled lectin. Nuclei were counterstained with Hoechst 33342. Scale bars = 100 μm. **B,C.** The area of the intimal and medial layers were measured, and the ratio of intimal-medial areas (I/M) was calculated. Stenosis ratio was calculated as a ratio of lumen area to total vessel area. Open bars; sham; closed bars: injury. **D.** Vascular medial explants of NG2-CreER/*Ninj1*^{loxp} mice were incubated in the presence or absence of hydroxy-tamoxifen (*Ninj1* KO or control, respectively). NG2^{+} cells were immunostained, and the number of vascular smooth muscle cells (either NG2^{+} and NG2^{-} cells) outgrowth from explants was counted. Scale bars = 50 μm. Values are presented as mean ± SEM. *P<0.05, **P<0.01 (n=5-9). n.s.: not significant.

Figure 5

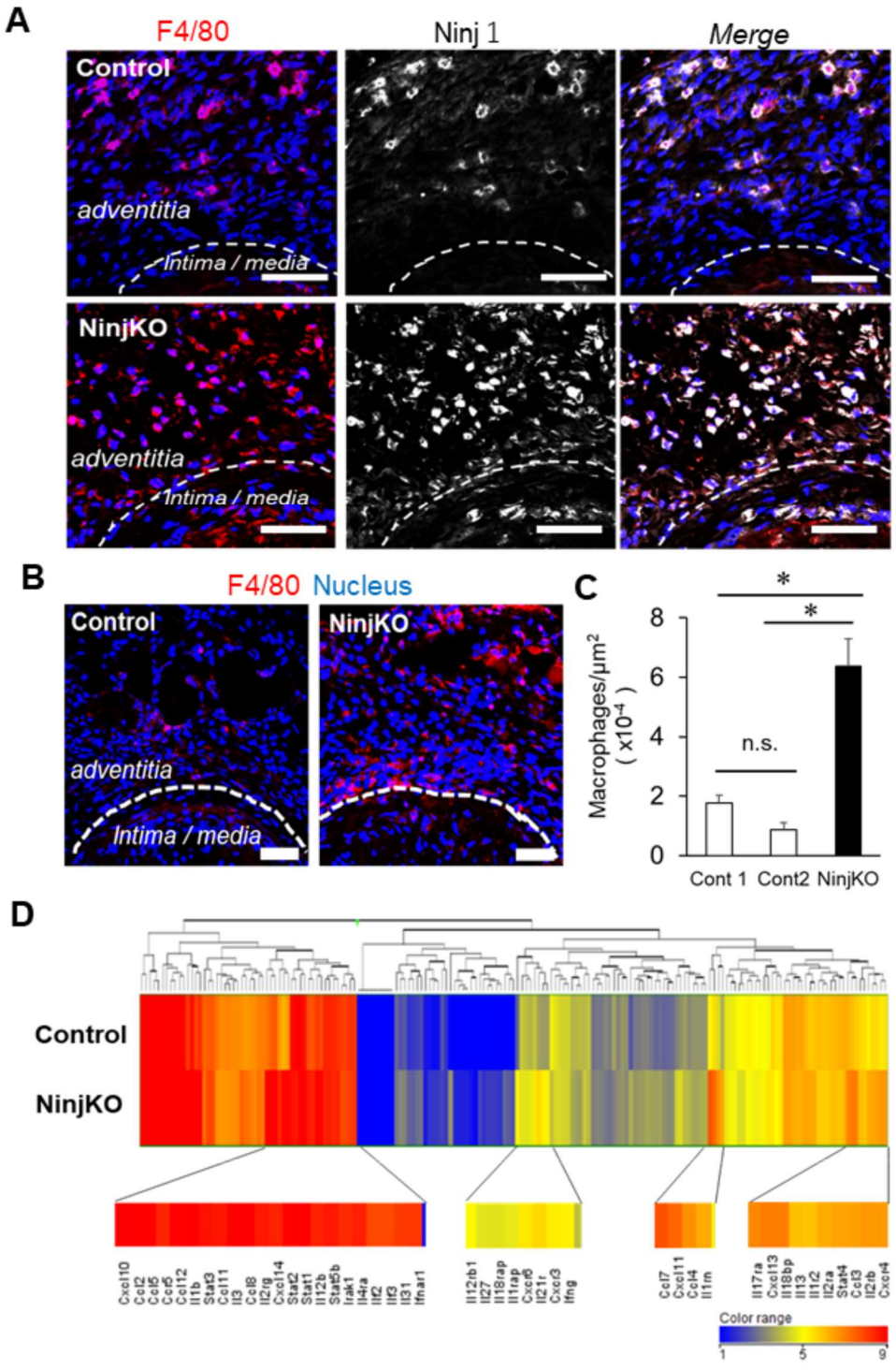
A
F4/80
Ninj 1
Merge
Control
adventitia
Intima / media
NinjKO
adventitia
Intima / media
B
F4/80 Nucleus
Control
adventitia
Intima / media
NinjKO
C
Macrophages/μm²
(x10⁻⁴)
8
6
4
2
0
*
*
n.s.
Cont 1
Cont2
NinjKO
D
Control
NinjKO
Cxcl10 Ccl2 Ccl5 Ccr5 Ccl12 Il1b Stat3 Ccl11 Il3 Ccl8 Il2rg Cxcl14 Stat2 Stat1 Il12b Stat5b Irak1 Il4ra Il2 Il5 Il31 Ifnar1
Il12rb1 Il27 Il18rap Il1rap Cxcr6 Il21r Cxcr3 Ifng
Ccl7 Cxcl11 Ccl4 Il1rn
Il17ra Cxcl13 Il18bp Il13 Il12 Il2ra Stat4 Ccl3 Il2rb Cxcr4
Color range
1
5
9

Figure 5. Effects of Ninj1 KO on macrophage infiltration in the adventitia of injured vasculature. A. At one week after vascular injury, short axis sections of femoral arteries of *Ninj1* KO and control mice were observed by immunostaining of F4/80$^+$ macrophages and Ninj1. **B**. At 4 weeks after vascular injury, short-axis view of injured vasculature with immunostained F4/80$^+$ cells. Nuclei were counterstained with Hoechst 33342. Scale bars =50 μm. **C**. The number of macrophages in the observed adventitial area was counted. **D.** Clustering analysis among genes related to inflammatory responses defined by GO analysis was performed using microarray gene expression in control and *Ninj1* KO mice. Values are presented as mean ± SEM. **P*<0.05 (n=6). n.s.: not significant.

Table 1 Gene expression profile of injured femoral arteries in Ninj1 KO and control mice.

Marker	Gene		Gene expression		
	symbol	*discription*	*Control*	*NinjKO*	*ratio*
EC	Pecam1	platelet/endothelial cell adhesion molecule 1	1679	1527	0.91
	Vcam1	vascular cell adhesion molecule 1	1390	1590	1.14
	vWF	Von Willebrand factor homolog	15	12	0.81
	CDH5	cadherin 5 (VE-cadherin)	27	18	0.66
PC	PDGFRβ	platelet derived growth factor receptor, β polypeptide	1157	1172	1.01
	NG2(CSPG4)	chondroitin sulfate proteoglycan 4	154	144	0.93
VSMC	**Acta2**	actin, alpha 2, smooth muscle, aorta	45633	15501	**0.34**
	Tagln	transgelin or smooth muscle 22a	16975	8198	**0.48**
	Myh11	smooth muscle myosin heavy chains	2420	2250	0.93
Angiogenesis	Angpt1	angiopoietin 1	132	125	0.95
	Angpt2	angiopoietin 2	1277	894	0.70
	VGEFa	vascular endothelial growth factor A	52	56	1.07
	VGEFb	vascular endothelial growth factor B	1111	999	0.90

Table 1 Gene expression profile of injured femoral arteries in Ninj1 KO and control mice.

Femoral arteries of Ninj1 KO and control mice were isolated 4 weeks after vascular injury, and microarray gene expression was compared between control and Ninj1 KO mice (three-independent samples). The detected signal for each gene was normalized using the global normalization method. The definition of a significant difference was more or less than twice the difference in the log2 ratio among genes with a fluorescence value >100 (shaded). EC: endothelial cell; PC: pericyte; VSMC: vascular smooth muscle cell.

Table 2.Gene expression profile regarding inflammation.

marker	*Gene*	*RefSeq ID*	*Control*	*NinjKO*	*Difference (ratio)*
Inflammatory cells	CD68	NR_110993.1	737	689	0.93
	CD74	NM_001042605.1	2233	4499	**2.02**
	CD163	NM_001170395.1	38	38	0.99
	TLR2	NM_011905.3	262	481	1.84
	TLR4	NM_021297.3	136	148	1.09
	STAT1	NM_001205313.1	237	528	**2.23**
	CCR2	NM_009915.2	263	696	**2.65**
	CCR5	NM_009917.5	97	351	**3.60**
	CCR7	NM_007719.2	8	20	**2.48**
	CXCR4	NM_009911.3	43	95	**2.21**
	AIF1	NM_019467.2	666	2154	**3.23**
cytokine/chemokine	**IL1β**	NM_008361.4	98	539	**5.52**
	IL6	NM_001314054.1	6	11	1.85
	IL10	NM_010548.2	26	29	1.12
	TNF	NM_001278601.1	16	37	**2.26**
	TGFβ1	NM_011577.2	40	57	1.42
	CCL2	NM_011333.3	187	759	**4.05**
	CCL4	NM_013652.2	22	107	**4.80**
	CCL5	NM_013653.3	204	656	**3.22**
	CCL7	NM_013654.3	34	214	**6.26**
	CCL12	NM_011331.2	75	511	**6.85**
	CXCL9	NM_008599.4	289	1376	**4.77**
	CXCL10	NM_021274.2	140	787	**5.62**
	CXCL11	NR_038116.1	47	170	**3.61**
	CXCL13	NM_018866.2	66	132	**2.01**

Table 2 Gene expression profile regarding inflammation.

Microarray gene expression in injured femoral arteries was compared between control and Ninj1 KO mice (three-independent sample). The definition of a significant difference was more or less than twice the difference in the log2 ratio among genes with a fluorescence value >100 (shaded).